1-7-2003

Formation and character of an ancient 19-m ice cover and underlying trapped brine in an "ice-sealed" east Antarctic lake

Peter T. Doran

Christian H. Fritsen

Christopher P. McKay

John C. Priscu

Edward E. Adams

Recommended Citation

Doran, P., Fritsen, C., McKay, C., Priscu, J., & Adams, E. (2003). Formation and character of an ancient 19-m ice cover and underlying trapped brine in an "ice-sealed" east Antarctic lake. *Proceedings of the National Academy of Sciences of the United States of America, 100* (1), 26-31. https://doi.org/10.1073/pnas.222680999

Formation and character of an ancient 19-m ice cover and underlying trapped brine in an "ice-sealed" east Antarctic lake

Peter T. Doran*†, Christian H. Fritsen‡, Christopher P. McKay§, John C. Priscu¶, and Edward E. Adams‖

*Department of Earth and Environmental Sciences, University of Illinois, 845 West Taylor Street, MS 186, Chicago, IL 60607; ‡Division of Earth and Ecosystem Sciences, Desert Research Institute, 2215 Raggio Parkway, Reno, NV 89512; §Space Science Division, National Aeronautics and Space Administration, Ames Research Center, Moffett Field, CA 94035; ¶Land Resources and Environmental Sciences, 334 Leon Johnson Hall, Montana State University, Bozeman, MT 59717; and ‖Department of Civil Engineering, Montana State University, Bozeman, MT 59717

Communicated by P. Buford Price, Jr., University of California, Berkeley, CA, November 8, 2002 (received for review August 22, 2002)

Lake Vida, one of the largest lakes in the McMurdo Dry Valleys of Antarctica, was previously believed to be shallow (<10 m) and frozen to its bed year-round. New ice-core analysis and temperature data show that beneath 19 m of ice is a water column composed of a NaCl brine with a salinity seven times that of seawater that remains liquid below −10°C. The ice cover thickens at both its base and surface, sealing concentrated brine beneath. The ice cover is stabilized by a negative feedback between ice growth and the freezing-point depression of the brine. The ice cover contains frozen microbial mats throughout that are viable after thawing and has a history that extends to at least 2,800 ^{14}C years B.P., suggesting that the brine has been isolated from the atmosphere for as long. To our knowledge, Lake Vida has the thickest subaerial lake ice cover recorded and may represent a previously undiscovered end-member lacustrine ecosystem on Earth.

The McMurdo Dry Valleys represent a cold desert, receiving <10 cm of snowfall annually and having mean annual temperatures ranging from −14.8 to −30°C on the valley floors (the latter value is from the Lake Vida meteorological station) (1). The existence of the numerous closed-basin lakes in the region results from the 3–6 weeks during the summer when the melting point of glacier ice is exceeded and ephemeral streams flow into the lakes. The lake area adjusts such that the average loss by ablation increases with influx of meltwater. As the meltwater input decreases, the lake area will diminish, and eventually it will evaporate/sublime completely, as has occurred in the past (2, 3). These perennially ice-covered lakes have long been studied as extreme biological environments (4–6). The liquid water columns of these lakes are substantial (up to 70 m deep) and range from fresh to 270 parts per thousand salinity and −5 to +24°C. The ice covers are 3–6 m thick and typically have little snow cover, which allows adequate light penetration to support photosynthesis in the ice cover, liquid water column, and benthos (6, 7). Another set of lakes in the McMurdo Dry Valleys has been presumed to be frozen to their beds (often referred to as "ice-block" lakes), a conclusion based largely on drill or dynamited holes made into the ice covers without accessing water (refs. 8 and 9; G. D. Clow, personal communication; and D. McKnight, personal communication). Lake Vida in Victoria Valley (77°23′S, 161°56′E) has been the most intriguing of the presumed ice-block lakes because it is also one of the largest lakes (6.8 km^2) in the region. We report results from a ground-penetrating radar (GPR) survey, ice-core analysis, and thermodynamic model based on ice temperature to show that the ice cover is thick (19 m), rich in old organic matter associated with ice sediment, and overlies a cold hypersaline brine.

Methods

Field Methods. A PulseEKKO 100 GPR unit with a 1,000-V transmitter and 50-MHz antennas was used in the lake survey. The survey was performed in November 1995 and consisted of a transverse parallel antenna layout collecting 32 stacks per trace at 1 trace per second in continuous mode. The resulting data were low-pass-filtered and plotted with only constant gain and no trace-to-trace averaging. Ice coring was done by using a Polar-Ice Coring Office (PICO) 4-inch electromechanical ice-coring rig. Long-term ice temperatures were collected with a Campbell Scientific (Logan, UT) CR10 data logger driving 107B thermistors inserted in the core hole. The hole was back-filled with deionized water and allowed to freeze. Surface ablation has been tracked by both wooden ablation stakes drilled into the ice cover and measurement of exposed thermistor wires.

Laboratory Methods. A Dionex DX-300 ion chromatograph was used for the major ion analyses. Salinity of the under-ice brine was calculated by using the Fortran program FREZCHEM (10, 11) based on the ice/brine chemistry and the temperature at the depth of the briny ice. Bacterial density was determined by epifluorescence direct counts of acridine orange-stained samples (6). Microalgal and cyanobacterial biomass was expressed as chlorophyll *a* determined via fluorescence of DMSO/acetone-extracted pigments (6). Metabolic potential was measured via the incorporation of radiolabeled CO_2, thymidine, and leucine on samples incubated at 1°C (6, 12). Radiocarbon additions were performed on subsamples of the melted ice at a different location from all other sample handling to prevent contamination of samples to be dated by using radiocarbon techniques. The photosynthetic rate was measured at 300 μmol of photons·m^{-2}·s^{-1}, an irradiance that saturates photosynthesis (12). Heterotrophic activity was measured in the dark.

Results and Discussion

Physical, Chemical, and Biological Properties of the Ice. GPR was attenuated at ≈19 m beneath the ice surface in Lake Vida, indicating an ice/saline-water interface at this depth (Fig. 1). Because GPR signals are absorbed by saline water, the depth of the water body (i.e., distance from the ice bottom to the lake bottom) could not be determined. Two cores (15.8 and 14 m long and 4 inches in diameter) were extracted from Lake Vida in October 1996, and a thermistor string was embedded in one borehole to monitor ice temperatures continuously. The extracted cores contained gas bubbles with hoar frost (which should contribute to light attenuation due to its faceted nature) below ≈6 m. At 15.8 m in the core, wet saline ice was encountered with a temperature of −11.6°C (Fig. 2). Brine trapped in the ice at the bottom of the core was determined to be dominantly NaCl with an inferred concentration of 245 parts per thousand or ≈7 times that of seawater. Major anions are: Cl^-, 80.2%; SO_4^{2-}, 18.8%; NO_3^-, 0.3%; F^-, 0.1%; and Br^-, 0.1%.

Abbreviation: GPR, ground-penetrating radar.

†To whom correspondence should be addressed. E-mail: pdoran@uic.edu.

www.pnas.org/cgi/doi/10.1073/pnas.222680999

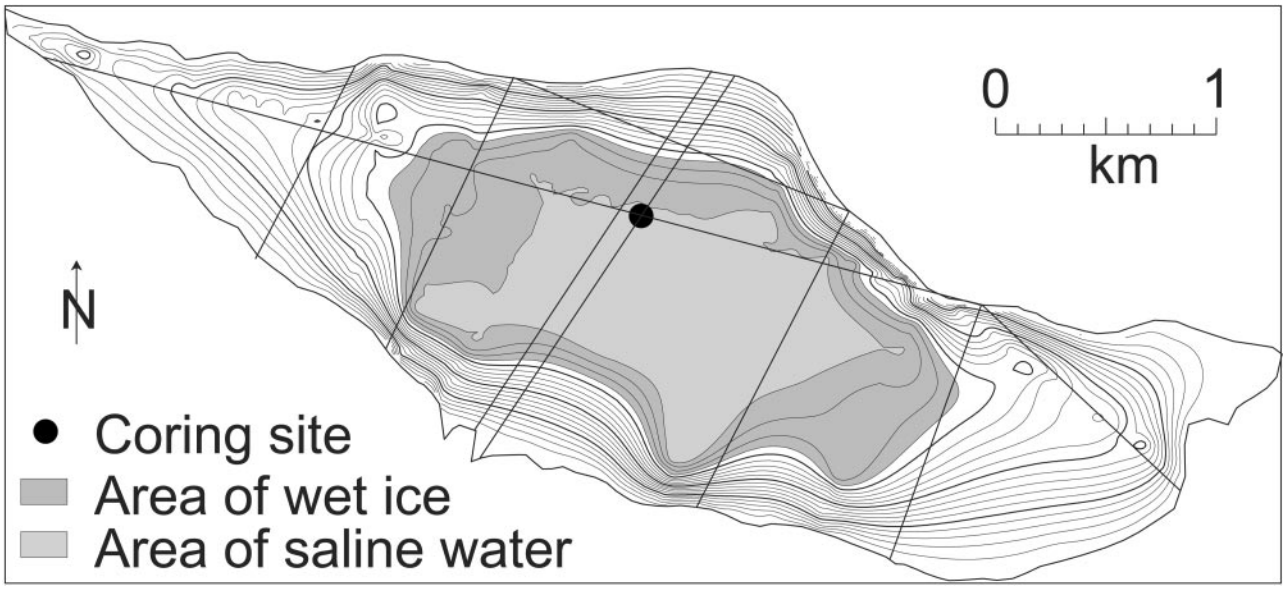

Fig. 1. Bathymetric map of Lake Vida. Isobaths are at 1-m intervals (thicker lines occur every 5 m) and interpreted from the GPR survey performed in November 1995 (survey lines are indicated). The saturated ice depth was determined during drilling.

Major cations are: Na^+, 67.2%; Mg^{2+}, 22.3%; K^+, 8.9%; and Ca^{2+}, 1.6%. It is noteworthy that the ratio of salts in the brine is very close to the ratio in some of the other McMurdo Dry Valley lakes (e.g., Lake Bonney; ref. 13), suggesting these lakes have a similar history of thick ice cover. Based on GPR, the deep briny ice in Lake Vida would have been 3–4 m above the primary ice/liquid water interface. Liquid did not rise in the borehole, indicating that we were not in hydrologic contact with the main brine body. From extrapolation of the measured temperatures in the ice cover we infer that the temperature at the main brine layer is ≈ -10°C. The GPR results show parabolic reflections in the ice starting at 16 m, which we interpret as the start of briny ice. The ice cores contained five cohesive sediment layers in the top 7 m with dispersed layers of microbial mats throughout the core (Fig. 2). Sleewaegen *et al.* (14) noted a similar sediment layer in the ice cover of a 4.8-m-deep ice-block lake and attributed it to aeolian processes. Our sediment layers presumably are formed by the flooding of the ice surface with turbid stream water. Sediment in this flood water settles into layers before the water freezes on top of the lake. The importance of this process became evident during the 2001/2002 (after our ice core was taken) high-flow season, when Lake Vida was covered by $\approx$1 m of extremely turbid water (J.C.P., personal observation). The sediment layers, in concert with high bubble density and the overall thickness of the ice, effectively block light from reaching the lower portions of the ice cover. Surface ice ablation measured annually since 1996 is negligible, implying that stream water flooding the ice surface in the summer, in combination with snow that often covers the ice (in contrast to other McMurdo Dry Valley lakes), roughly balances evaporative loss in most years. During high-flow years, ice accumulates on the surface, giving an apparent negative annual ablation.

Profiles of microbial biomass in the ice cores indicate that heterotrophic and photoautotrophic cells (primarily filamentous cyanobacteria) are associated with sedimentary material within the ice matrices (Fig. 2). Computed tomography x-ray scans of solid ice cores with sediment inclusions surrounded by the mats verified this close association. Microbial assays performed on ice-core meltwater from 0 to 12 m demonstrated that both heterotrophic and photoautotrophic cells retain metabolic potential after thawing. These metabolic results show that ice-bound microbial populations are capable of growth if liquid water were to become available on either macro- or microscales within the permanent ice environment, corroborating studies conducted on other ice microbial assemblages within the dry valleys (6, 12). Two radiocarbon dates obtained from organic material in the ice core indicate that the ice and associated microbes are up to 2,800 ^{14}C years old 12 m beneath the surface (Fig. 2).

The subzero temperatures in the brine are highly restrictive to metabolic processes and are close to the lower limits where microbial activity has been observed (15, 16). The inferred high solute concentration is likely to be an additional constraint on microbial activity, but the water activity ($\approx$0.79) is well above the water activity of 0.62 that is believed to be the limit for microbial growth (17, 18). Therefore, the inferred physical environment within the brine appears restrictive but does not preclude the possibility of active microbes. The energy and carbon sources to sustain active populations of microbes are likely to be limited because the thick sediment and bubble-laden ice overlying the brine will limit contemporaneous photoautotrophy.

Thermal Analysis and Modeling. Ice temperatures, together with meteorological observations made at the surface, allowed us to model the thermal evolution of Lake Vida over a 4-year period. Instantaneous and mean annual ice temperatures (Fig. 3) have been decreasing at all depths over the time of the observations.

In addition, the average temperature gradient in the ice cover results in a net annual upward heat flow of $\approx$0.7 $W \cdot m^{-2}$. The mean annual temperature at the meteorological station on the shore of Lake Vida averaged -27.4°C (range, -25.9 to -30.1°C) from 1996 to 2000 (1). During this same period the mean annual temperatures at Lake Hoare in Taylor Valley averaged -17.7°C (range, -16.1 to -19.2°C) and at Lake Vanda in Wright Valley averaged -19.3°C (range, -18.3 to -22.4°C) (1). The record at the nearby Lake Hoare station indicates that the region has been undergoing cooling, particularly during the summer months, between 1986 and 2000 (19). The temperature gradient determined from the bottom two temperature sensors shows that that ice freezes and melts from the bottom of the ice cover alternately with the summer and winter seasons. The time of maximum freezing at the bottom of the ice corresponds to the warmest air

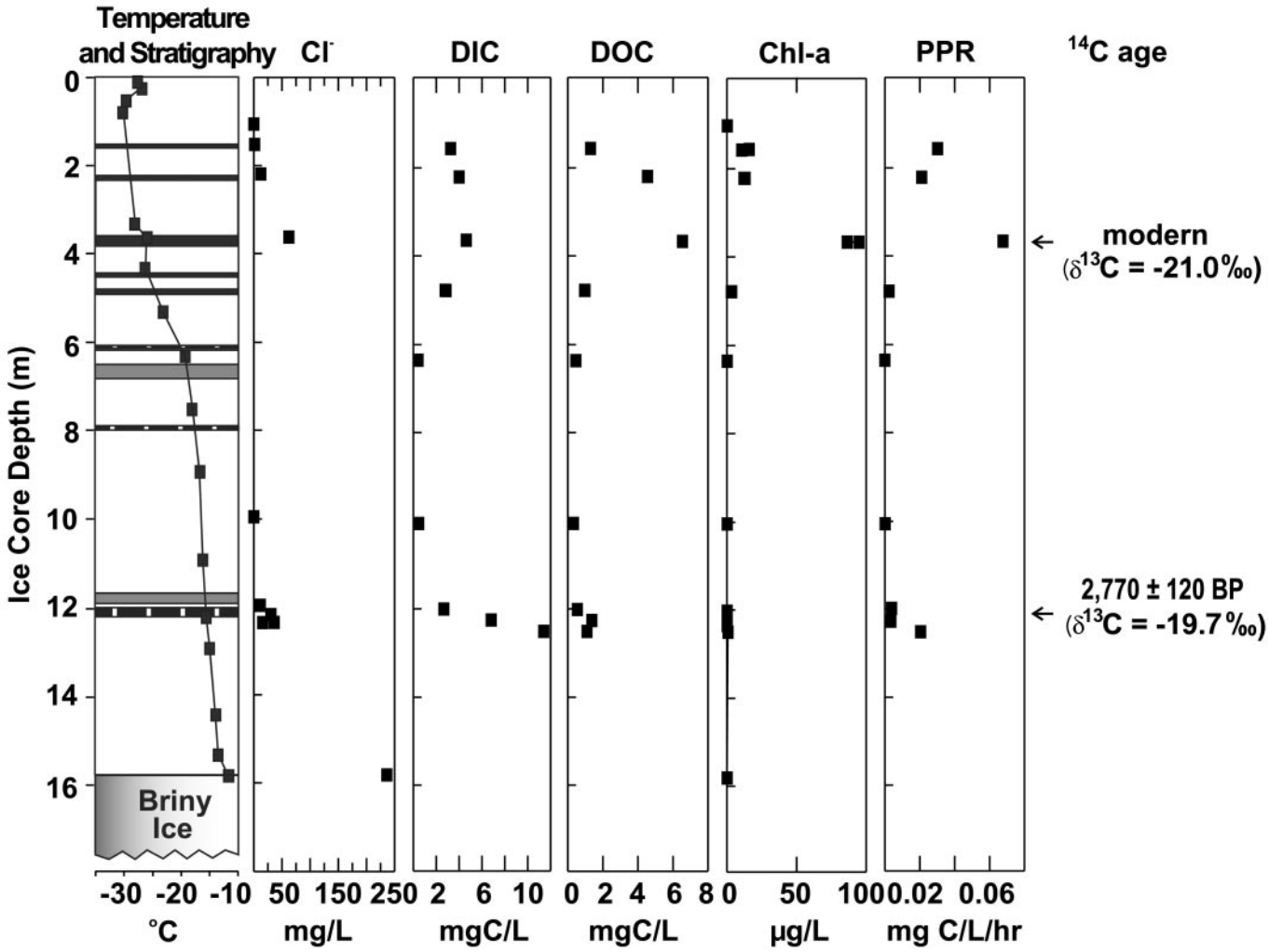

Fig. 2. Physical and chemical properties of a Lake Vida ice core extracted in October 1996. Black horizons on the stratigraphy plot represent sediment layers, gray horizons are sandy ice, and vertically banded horizons contain microbial mat. The temperature profile was taken at the time of the core extraction. PPR, primary productivity; DIC, dissolved inorganic matter; DOC, dissolved organic matter; Chl-a, chlorophyll *a*.

temperature (i.e., summer), with a net excess of freezing over melting by ≈7cm/year.

We have modeled the temperature in the ice by the analytical expression for the ground temperature in a semi-infinite uniform solid experiencing sinusoidal surface temperature variations (20).

$$T(z, t) = T_0 + \alpha z + \Delta T e^{-z/\delta} \sin(\omega t - z/\delta) \qquad [1]$$

where T_0 is the mean annual temperature at the surface, z is the depth taken as positive downward, α is the average annual temperature gradient due to the average annual heat flow through the ice cover (resulting from geothermal heat or ice formation at the bottom of the ice cover), ω is the frequency of the annual wave ($\omega = 2\pi$/year), ΔT is the amplitude of the seasonal temperature variation ($\Delta T \approx 30$°C at Lake Vida), and δ is the depth of penetration (damping depth) of the annual thermal wave given by $\delta = \sqrt{(2k/\omega\rho c)}$, where ρ is the density of the ice (900 kg·m^{-3}), k is the thermal conductivity of ice (2.4 W·m^{-1}·K^{-1} at $T \approx -10$°C), and c is the heat capacity (2,000 J·kg^{-1}·K^{-1}). Note that Eq. **1** averages over the effects of latent heat due to melting and freezing within the ice cover. Comparing the phase of the wave with depth and the attenuation of the amplitude with depth shows that the data are well represented by Eq. **1** for a damping depth of ≈4 m, close to the theoretical value for ice of 3.65 m (Fig. 4). The average net annual temperature gradient, α, is 0.3 K/m (Fig. 3), which implies a net annual average heat flow of 0.7 W·m^{-2}. If this heat flow were due to latent heat released by freezing, it would correspond to a freezing rate of 7 cm·year^{-1} (latent heat = 3.34×10^5 J·kg^{-1}).

The seasonal delay of ice formation and melting at the bottom of the ice cover relative to the surface temperature, evident in Fig. 1, can be understood by using Eq. **1**. The time dependence of the downward heat flow (presumed due to melting of ice) at the bottom of the ice is proportional to $-dT/dz$, which for any given position can be determined directly from the derivative of Eq. **1** as

$$-dT/dz = -\alpha + (\Delta T/\delta) e^{-z/\delta} [\sin(\omega t - z/\delta) + \cos(\omega t - z/\delta)]. \qquad [2]$$

The right hand side of Eq. **2** is a sum of sine and cosine, and its maximum occurs one-eighth of a cycle (45° or $\pi/4$ radians) before the maximum of a simple sine wave (Eq. **1**). Thus the phase, $\Theta(z)$, of maximum downward heat flow (ice melting) with depth is given by $\Theta(z) = z/\delta - \pi/4$.

As an example, if we take 12 m as the average depth between the bottom two layers for which we have measurements and for

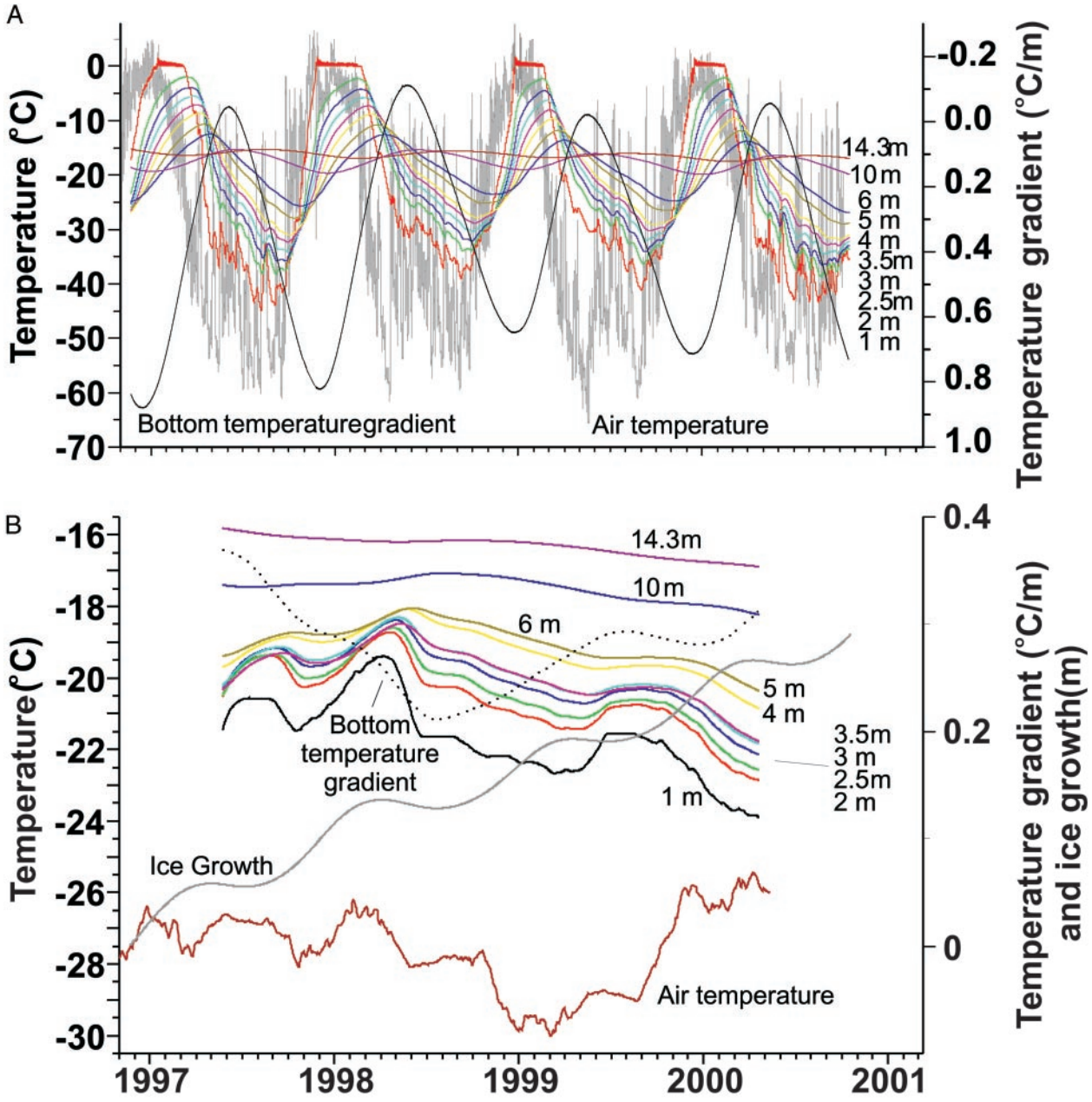

Fig. 3. (*A*) Ice temperatures, air temperature, and temperature gradients from Lake Vida over time. (*B*) Running mean annual ice temperatures, air temperature, calculated heat gradient using the bottom two thermistors (10 and 14.3 m), and modeled ice growth at the base of the ice cover.

$\delta = 4$ m, we would expect the maximum in downward heat flow at 12 m to be 2.2 radians, or 0.35 years (129 days), after the temperature maximum at the surface. This relative phase is in good agreement with the relative phase of the air temperature and the bottom flux shown in Fig. 3. Note that ice melting is maximum for negative values of the bottom flux. Thus, the melting at the bottom (negative bottom flux) of the thick ice on Lake Vida peaks in the winter, and the freezing (positive bottom flux) peaks in the summer. This phase reversal has not been observed on the thinner ice covers of the other lakes, because for ice covers of between 4 and 6 m in thickness, the phase delay between summer at the surface and maximum melting of ice is only 12.5 and 42 days, respectively.

The previous discussion shows that the ice on Lake Vida is thick enough that its response time is comparable to 1 year, which allows us to model the response of the ice cover to multiyear variations in climate by using an annually averaged model. Thus for a specified mean annual air temperature, we used an annual averaged thermal balance model for the ice cover to determine the expected thickness of the ice. Ice growth or melt is inferred by comparing the computed ice thickness from the model under different conditions. For example if under one temperature regime the predicted ice thickness was 19 m and under another regime 3 years later it was 21 m, we would use the model to predict an ice growth rate of 1 m/year. In this way we use the time-independent annual-average model to help understand the time behavior of the lake ice.

The model we use is based on McKay *et al.* (21), with the albedo set to 0.3 and only the solar flux in the visible assumed to enter the lake (half the solar constant) as suggested by ref. 22.

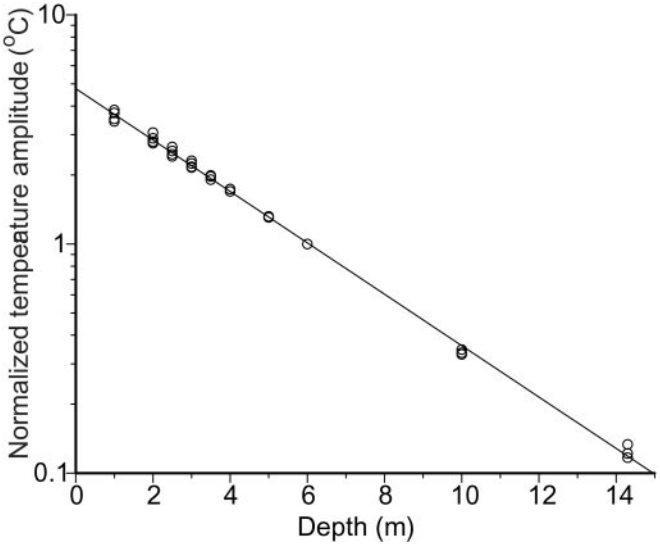

Fig. 4. Temperature amplitude for each year of the data set normalized to the amplitude at 6 m for that same year. The least-squares line gives a damping depth of 3.8 m.

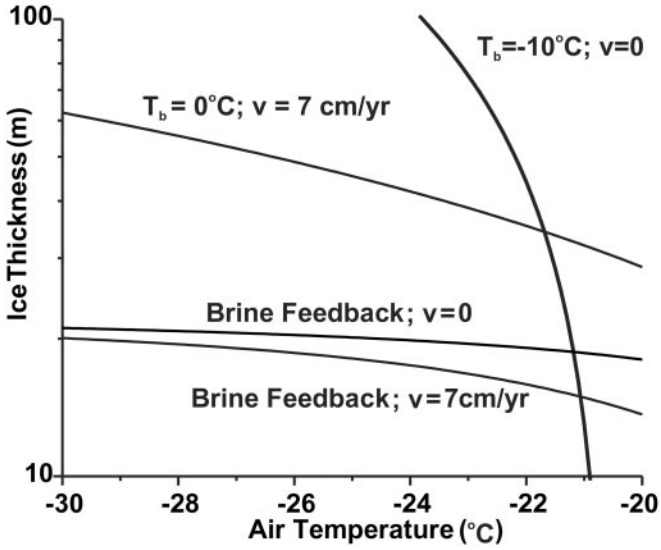

Fig. 5. Ice thickness computed from energy-balance model as described in Thermal Analysis and Modeling. Curves are shown for the lower boundary condition for brine ($T_b = -10$°C) and no heat flow, fresh water ($T_b = 0$°C), and heat flow corresponding to 7 cm/year of ice formation, and for the lower boundary determined by a brine feedback in which the temperature of the lower boundary varies as the concentration of the brine changes because of ice formation. Curves with brine feedback with and without heat flow are shown.

We use only the flux in the visible because measurements of the transmission of the lake ice show that only visible radiation (below 700 nm) penetrates the ice (23). Our value for the albedo in this wavelength region is based on direct measurements over the lake ice (23). As in McKay *et al.* (21), the ice cover is treated as uniform with an attenuation of visible light in the ice such that 1 optical depth corresponds to a length of 0.8 m, and 10% of the ice surface is assumed to be covered with dark material. Previous applications of this model to the McMurdo Dry Valley lakes (21) have assumed constant temperature (usually 0°C) at the lower boundary and a heat flux due to freezing of ice at the bottom of the ice cover to balance ablation from the top of the ice cover. We initially computed the thickness of the ice expected if the only heat flow was geothermal heat (0.08 $W \cdot m^{-2}$ based on measurements at several sites in the region; ref. 24), and the temperature at the bottom of the ice cover was constant at −10°C, the estimated temperature in the main brine layer. In this case, the thickness of the ice increases markedly for mean annual air temperatures below −21°C (Fig. 5). We then computed the expected thickness for a constant lower boundary temperature of 0°C but with the observed heat flux corresponding to an ice growth rate of 7 cm/year. In this case, the calculated ice thickness was always much larger than observed (Fig. 5).

To simulate the effect of the changing salinity and freezing point as the ice thickens we modified the model to include brine feedback. From the bathymetry of the lake (Fig. 1) we estimate the thickness of the brine layer to be ≈5 m. Based on our initial temperature observation we considered that the 5-m brine layer was in equilibrium with a layer of ice 19 m thick at a brine temperature of −10°C. The mean annual air temperature at which this configuration would be stable is −23°C. Allowing the ice thickness to increase or decrease, we then computed the increase or decrease in the brine-layer thickness and the new freezing point of the brine solution. The results for two cases of ice-growth rate, 0 and 7 cm/year, are shown in Fig. 5. The stability of the ice evident in these curves is the result of the change of the freezing point of the brine. For example, for the ice-growth rate of 7 cm/year, the freezing point of the brine when the air temperature is −20°C (ice thickness is 13.5 m) is −5°C, whereas at an air temperature of −30°C (ice thickness is 20 m) the freezing point is −12.3°C. Thus the brine layer acts as a negative feedback on the ice thickness with respect to air temperature and ice growth. The observed heat flux (corresponding to 7 cm of ice/year) can be explained if we assume that the lake was in equilibrium with an air temperature of −21°C and then recently was exposed to an air temperature of −28°C. This is a plausible scenario given the general cooling the McMurdo Dry Valleys have undergone in the last 14 years (19) and the role that winter winds play in determining the mean annual temperature at Lake Vida (1).

In our proposed scenario for the lake ice, the initial equilibrium state corresponds to an air temperature of −23°C, ice thickness of 19 m, brine depth of 5 m, and brine temperature of −10°C for a heat flow of 0.08 $W \cdot m^{-2}$ (geothermal only). We now assume that the air temperature cools to −28°C (mimicking recent temperature trends at Lake Vida). Now that the ice cover is no longer in equilibrium, the new equilibrium would have an ice thickness of 21 m, brine depth of 3 m, and brine temperature of −16°C, for a heat flow of 0.08 $W \cdot m^{-2}$ (geothermal only). Note that the brine is now 1.5 times more concentrated than in the initial state due to the reduction in fluid volume. However, for the new equilibrium to be reached, 2 m of new ice must grow at the bottom of the ice cover (no associated ablation is implied). For this to occur, the latent heat of these 2 m must be conducted out of the ice cover. For the cases chosen here, ≈7 cm of ice will form each year. When the ice cover is still in its initial state of 19 m and the brine temperature is −10°C but the air temperature has become −28°C, then the perturbed system can only be in steady state if the heat flow through the ice is equivalent to ≈7 $cm \cdot year^{-1}$ of new ice. These results are approximate because we have used a steady-state model to estimate the rate of transition between equilibrium states. However, if the time scale for the ice to come to thermal adjustment is short compared with the time for the transition from the initial steady state to the final steady state, then this approximation is reasonable. Further assumptions include: (*i*) latent heat independent of salinity and (*ii*) the volume of the brine layer is assumed to be simply proportional to its depth, ignoring any change in area of the brine with depth.

Also untested in this hypothesis is that the temperature at Lake Vida was ≈ -23°C before the period of observation.

Conclusions

Lake Vida represents an aquatic ecosystem that is the result of an unusual combination of summers warm enough to generate melt from local glaciers and winters cold enough to create a sufficiently thick ice cover to keep the meltwater from flowing below the ice. The depth of summer-soil thaw inferred from thermistors buried on the northwest shore of Lake Vida is often <25 cm and even in some of the warmest summers on record (e.g., 2001/2002) only barely exceeds 50 cm. As shown in Fig. 2, the Lake Vida ice cover remains frozen year-round below 2 m depth, and we see no evidence of brine drainage in the ice cores. These conditions create what can be best labeled as an ''ice-sealed'' lake, which distinguishes Lake Vida from the other perennially ice-covered lakes that receive meltwater below the floating ice cover and exchange gases with the atmosphere annually. Our analysis indicates that Lake Vida has been in this ice-sealed mode for at least 2,800 ^{14}C years with the bottom of the ice cover adjusting in thickness and the brine changing in salinity as a response to changes in the local climate. Sediment layers in the top 7 m of the ice cover indicate that significant summer floods have been more frequent in the recent history of the lake. Thick layers of water can form below the ice surface in moderately warm summers (25), which provides the potential for settling and redistribution of sediment through the surface layers of ice. However, we are unaware of a mechanism that could move sediment downward through the bottom of this thick ice, leading us to conclude that Lake Vida is currently undergoing a clastic sedimentation hiatus that will be represented in the sediment record as a period restricted to salt deposition and dissolution.

Lake Vida provides a unique model for understanding what may have happened to other lakes during severe climactic deteriorations of the past. For instance, if large subglacial lakes such as Lake Vostok had existed without overlying glacial ice before glaciation, they would have shifted into this ice-sealed mode just before being over-ridden by glaciers. Lake Vida currently is poised very close to the regional snow line, a condition that would occur in a periglacial Lake Vostok. A preglacial sediment record in Lake Vostok will depend on the extent of sediment scouring by advancing glaciers (26), and the Lake Vida model would provide a mechanism for protecting this record. After sufficient glacial ice accumulation, melting would occur at the glacier base, diluting any salts present. Even lakes in more temperate settings today may have followed the path of Lake Vida during a transition into a severe glacial period (e.g., during the Neoproterozoic; ref. 27). Finally, Lake Vida may represent an analog of the last vestige for ancient Martian aquatic ecosystems, because Mars cooled after a warmer and wetter past (28).

We thank J. Schmok for carrying out the GPR survey, K. Welch for performing major ion analysis, and D. Gilles for supervising the ice coring. This work was supported by National Science Foundation Grants OPP-9211773, OPP-9419413, OPP-9814972, and OPP-0085400 and National Aeronautics and Space Administration Exobiology Grants NAGW-1947 and NAG5-9889.

1. Doran, P. T., McKay, C. P., Clow, G. D., Dana, G. L., Fountain, A. & Nylen, T. (2003) *J. Geophys. Res.*, in press.
2. Wilson, A. T. (1964) *Nature* **201,** 176–177.
3. Lyons, W. B., Tyler, S. W., Wharton, R. A., McKnight, D. M. & Vaughn, B. H. (1998) *Antarct. Sci.* **10,** 247–256.
4. Parker, B. C., Seaburg, K. G., Cathey, D. D. & Allnutt, F. T. C. (1982) *J. Plankton Res.* **4,** 271–286.
5. Spaulding, S. A., McKnight, D. M., Stoermer, E. F. & Doran, P. T. (1997) *J. Paleolimnol.* **17,** 403–420.
6. Priscu, J. C., Fritsen, C. H., Adams, E. E., Giovannoni, S. J., Paerl, H. W., McKay, C. P., Doran, P. T., Gordon, D. A., Lanoil, B. D. & Pinckney, J. L. (1998) *Science* **280,** 2095–2098.
7. Green, W. J. & Friedmann, E. I. (1993) in *Antarctic Research Series* (Am. Geophys. Union, Washington, DC), Vol. 59, pp. xi, 216.
8. Calkin, P. E. & Bull, C. (1967) *J. Glaciol.* **6,** 833–836.
9. Hendy, C. H. (2000) *Geografiska Annaler Ser. A Phys. Geogr.* **82A,** 411–432.
10. Marion, G. M. & Grant, S. A. (1994) FREZCHEM: A Chemical-Thermodynamic Model for Aqueous Solutions at Subzero Temperatures (Cold Regions Res. Eng. Lab., U.S. Army Corp of Engineers, Hanover, NH).
11. Marion, G. M. (1997) *Antarct. Sci.* **9,** 92–99.
12. Fritsen, C. H. & Priscu, J. C. (1998) *J. Phycol.* **34,** 587–597.
13. Spigel, R. H. & Priscu, J. C. (1996) *Hydrobiologia* **321,** 177–190.
14. Sleewaegen, S., Lorrain, R., Offer, Z., Azmon, E., Fitzsimons, S. & Souchez, R. (2002) *Earth Surf. Processes Landforms* **27,** 307–315.
15. Baross, J. A. & Morita, R. Y. (1978) in *Microbial Life in Extreme Environments*, ed. Kushner, D. J. (Academic, New York), pp. 9–71.
16. Herbert, R. A. (1986) in *Microbes in Extreme Environments*, eds. Herbert, R. A. & Codd, A. A. (Academic, London), pp. 1–23.
17. Kushner, D. J. (1978) in *Microbial Life in Extreme Environments*, ed. Kushner, D. J. (Academic, New York).
18. Brown, A. D. (1990) *Microbial Water Stress Physiology: Principles and Perspectives* (Wiley, New York).
19. Doran, P. T., Poiscu, J. C., Lyons, W. B., Walsh, J. E., Fountain, A. G., McKnight, D. M., Moorhead, D. L., Virginia, R. A., Wall, D. H., Clow, G. D., *et al.* (2002) *Nature* **415,** 517–520.
20. Campbell, G. S. (1977) *An Introduction to Environmental Biophysics* (Springer, New York).
21. McKay, C. P., Clow, G. D., Wharton, R. A. & Squyres, S. W. (1985) *Nature* **313,** 561–562.
22. Warren, S. G., Brandt, R. E., Grenfell, T. C. & McKay, C. P. (2002) *J. Geophys. Res.* **107,** 3167.
23. McKay, C. P., Clow, G. D., Andersen, D. T. & Wharton, R. A. (1994) *J. Geophys. Res. Oceans* **99,** 20427–20444.
24. Decker, E. R. & Bucker, G. J. (1977) *Antarct. J. US* **XII,** 102–104.
25. Webster, J. G., Brown, K. L. & Vincent, W. F. (1994) *Hydrobiologia* **281,** 171–186.
26. Siegert, M. J., Ellis-Evans, J. C., Tranter, M., Mayer, C., Petit, J. R., Salamatin, A. & Priscu, J. C. (2001) *Nature* **414,** 603–609.
27. Hoffman, P. F., Kaufman, A. J., Halverson, G. P. & Schrag, D. P. (1998) *Science* **281,** 1342–1346.
28. McKay, C. P. (1997) *Origins Life Evol. Biosphere* **27,** 263–289.